Flux Decline in Nanofiltration Due to Adsorption of Dissolved Organic Compounds: Model Prediction of Time Dependency

Leen Braeken, Bart Van der Bruggen,* and Carlo Vandecasteele

Laboratory for Applied Physical Chemistry and Environmental Technology, Department of Chemical Engineering, Faculty of Engineering, K.U. Leuven, W. de Croylaan 46, 3001 Leuven, Belgium

Received: June 24, 2005; In Final Form: October 4, 2005

Flux decline during nanofiltration of aqueous solutions containing dissolved organic compounds is mainly caused by adsorption of these compounds in the membrane pores and on the membrane surface. In this paper, flux decline is modeled by incorporating the loss of permeability due to adsorption in the Spiegler−Kedem equation. This results in a logarithmic relation between normalized flux decline and time until the adsorption equilibrium is reached and the flux reaches a constant value. In this way, the expected flux decline due to adsorption of organic compounds can be estimated. Two different parameters were used in the model: the time delay t_0, which corresponds to the time at which the adsorption process in the membrane pores and on the membrane surface sets in, and the corresponding reduction of free (pore) volume (b). Both parameters depend on the hydrophobicity of the compounds and on the feed concentration.

1. Introduction

Nanofiltration is a pressure-driven membrane process used for the simultaneous removal of large to relatively small organic molecules (molar mass between 200 and 1000, depending on the pore size) and multivalent ions from process water or wastewater. Applications have already been realized, mainly in the drinking water industry.[1−3] However, one of the major drawbacks for the implementation of nanofiltration in industrial processes is the occurrence of fouling, which affects the retention of organic compounds and results in flux decline.

Flux decline causes practical problems in the application of nanofiltration: for a given membrane surface, the yield of permeate decreases, the energy consumption increases because higher pressures are needed to obtain the same flow rate, cleaning procedures need additional chemical reagents, and the lifetime of the membrane decreases. Fouling might also influence the retention of organic compounds.[4−6]

It is usually accepted that flux decline in aqueous solutions containing organic molecules is mainly caused by adsorption, possibly enhanced by pore blocking.[7,8] Adsorption on nanofiltration membranes has also been related to high performance liquid chromatography (HPLC) characteristics.[9,10] Earlier studies also show an influence of the hydrophobicity of a dissolved organic compound, represented by log P, on flux decline.[7]

The aim of this research is to describe the evolution of flux decline as a function of time based on the adsorption behavior of the dissolved organic compounds; adsorption in the pores and on the membrane surface results in a reduction of the pore size and thus a reduction of the membrane permeability. Other effects due to the presence of NOM,[11] Ca ions,[12] etc. were not taken into account.

* Corresponding author. E-mail: Bart.vanderbruggen@cit.kuleuven.be; Tel: +32 (0)16 32 23 40; Fax: +32 (0) 16 32 29 91.

2. Experimental Methods

Membranes, Membrane Characterization, and Filtration Experiments. Four different membranes were used: UTC-20 (Toray Ind. Inc., Shiga, Japan), Desal HL-51 (Osmonics SA, Vista, CA), NF210 (Dow-Filmtec, Edina, MN), and NTR-7450 (Nitto Denko, Tokyo, Japan). Table 1 summarizes the main properties of these membranes. The membranes used were different material-wise (three membranes are made of polyamide, one is made of polyethersulfon), but the MWCO values of two of the membranes used were quite similar. Specific interactions with the membrane material might have an influence, which should be reflected in the obtained model parameters.

Contact angle measurements were performed with a Krüss DSA 10 setup in a three-phase system consisting of membrane surface, air, and a drop of water. The sessile drop method was chosen. Each contact angle was measured 10 to 15 times and an average value was calculated. The contact angle of the wet, clean membrane was determined for all membranes.

Membrane charge was determined based on streaming potential measurements. The experimental setup has been described previously.[13] Based on the streaming streaming potential ΔE, the zeta potential ζ was calculated using the Helmholtz−Smoluchowski equation, with the Fairbrother and Mastin approach:

$$\zeta = \frac{\Delta E\, \eta\, \kappa_s}{\Delta P\, \epsilon} \tag{1}$$

where ΔP is the applied pressure, ϵ the dielectric constant, η the viscosity of the solution, and κ_s the specific conductivity. Based on the zeta potential ζ, the surface potential ψ can be calculated using the Eversole and Boardman equation (2), with e being the electronic charge, k the Boltzmann constant, z the valency of the counterions, T the temperature (K), κ the

10.1021/jp0534333 CCC: $33.50
Published on Web 01/21/2006

TABLE 1: Overview of Membrane Parameters

	UTC-20	Desal-HL-51	NTR 7450	NF270
Membrane material[a]	polypiperazineamide	polyamide	sulfonated polyethersulfon	polyamide
MWCO[a]	180	150−300	600−800	180
pH range[a]	3−10	3−9	2−11	3−10
Permeability ($l\ m^{-2}\ h^{-1}\ bar^{-1}$)[a]	15	9	12	11
Contact angle (°)	36	42	70	26
Membrane surface density (10^{-3} C/m^2) at pH = 7	−5.21	−9.17	−10.95	−14.91

[a] As specified by the manufacturers.

reciprocal of the Debye length (nm^{-1}), and δ the distance from the surface to the shearplane, which was set equal to 0.2 nm.[14]

$$\ln \tanh\left(\frac{ze\zeta}{4kT}\right) = \ln \tanh\left(\frac{ze\psi}{4kT}\right) - \kappa\delta \tag{2}$$

The Debye length λ_{deb} can be calculated according to eqs 3 and 4:

$$\lambda_{deb} = \sqrt{\frac{\epsilon RT}{2F^2 I}} \tag{3}$$

$$I = \frac{1}{2}\sum_i z_i^2 C_i \tag{4}$$

with R the ideal gas constant, T the temperature (K), F Faraday's constant, and I the ionic strength (eq 4).

The surface charge density σ_S was calculated using eq 5:

$$\sigma_S = \frac{\epsilon\,\psi}{\lambda_{deb}} \tag{5}$$

with ϵ the dielectric conductivity and λ_{deb} the Debye length. Equation 5 is valid only at low values of the zeta potential (<25 mV). At higher values of ζ, the Gouy−Chapman theory should be used, which is presented in eq 6. The difference in obtained surface charge density between both equations was for most membranes beneath 2.5%. Only for NF270 at pH 7 and 11 a difference of respectively 3.2% and 4.8% was obtained.

$$\frac{ze\psi}{2kT} = \text{arc sinh}\left(\frac{ez\sigma_S\lambda_{deb}}{2\epsilon kT}\right) \tag{6}$$

Nanofiltration experiments were performed using cross-flow equipment on laboratory scale.[10] Flat sheet membranes with an effective membrane area of 0.0059 m^2 were used. Permeate and retentate were recycled to the feed solution to obtain a constant feed concentration. The retention of a dissolved organic compound was calculated according to eq 7:

$$R = 1 - \frac{c_P}{c_F} \tag{7}$$

Before the experiments, the membranes were washed with distilled water to remove the protective coat and were pressurized during 1 h at 20 bar to avoid an influence of compaction on the flux measurements. A new membrane was used for each experiment. In all experiments, the temperature of the water was 25 °C and the transmembrane pressure was held at 8 bar.

Analysis. Table 2 summarizes the different compounds used in this research with their molecular weight and the logarithm of the octanol water partition coefficienct (log P). Samples containing a single compound with an aromatic structure (benzilidene acetone; 3,5-dihydroxybenzoic acid; 3,4 methylnitrofenol; *p*-tolualdehyde; benzaldehyde; and benzonitrile) in distilled water were analyzed by measuring UV absorption with a Shimazu UV 1601 double beam spectrophotometer. Table 3 gives the wavelengths used. Triethylene glycol, diethylene glycol, and diethanolamine were determined by using a HP 5890 Series II gas chromatograph equipped with a wide bore liquid-phase DB-1 (dimethyl polysiloxane) column with a film thickness of 5 μm. Cyclohexanone was measured using a Shimadzu GC-14A chromatograph equipped with a 80/120 mesh carbopack B/3% Sp-1500 column. Detection after the chromatographic separation occurred with a flame ionization detector (FID). Detector and injector temperature were 300 °C in all methods. A Waters TM 600S controller equipped with a Waters TM 626 pump was used to determine tartaric acid by HPLC using a Shodex RS pack KC-811 column with a length of 300 mm and an inner diameter of 8 mm. For the detection, a Waters 486 MS Tunable Absorbance Detector was used at a wavelength of 254 nm.

TABLE 2: Compounds Used with Their Molecular Weight and log *P*

component	molecular weight	log *P*
benzaldehyde	146	0.23
benzonitrile	103	1.54
benzilidene acetone	146	2.04
cyclohexanone	98	1.13
3,5-dihydroxybenzoic acid	154	0.91
diethylene glycol	106	−1.47
diethanolamine	105	−1.71
3,4-methylnitrophenol	153	2.45
p-tolualdehyde	120	2.26
tartaric acid	150	−1.00
triethylene glycol	150	−1.75

TABLE 3: Wavelengths Used in UV Spectrophotometry

component	wavelength λ (nm)
benzaldehyde	246.8
benzonitrile	224.0
benzilidene acetone	290.6
3,5-dihydroxybenzoic acid	210.0
3,4-methylnitrophenol	210.0
p-tolualdehyde	261.2

Error Calculation. The error on the model parameters was estimated by lineair regression on the data points (x_i,y_i). The correlation coefficient R^2 was calculated using the least-squares method. Based on R^2, the relative (δ) and absolute (Δ) error on intercept ($a = b \ln t_0$) and slope (b) were calculated using the following equations:

$$\Delta b = b\left[\frac{1}{n-2}\left(\frac{1}{R^2} - 1\right)\right]^{1/2} \tag{8}$$

$$\Delta a = \Delta b\left[\frac{1}{n}\sum_i (x_i^2)\right]^{1/2} \quad (9)$$

$$\delta b = \left[\frac{1}{n-2}\left(\frac{1}{R^2}-1\right)\right]^{1/2} \quad (10)$$

$$\delta a = \frac{\Delta b\left[\frac{1}{n}\sum_i (x_i^2)\right]^{1/2}}{a} \quad (11)$$

$$\delta(\ln t_0) = \sqrt{(\delta a)^2 + (\delta b)^2} \quad (12)$$

3. Theoretical Basis

Adsorption as a Function of Time. At a heterogeneous surface, adsorption sites are occupied in the order of increasing activation energy of the sites. The heterogeneity of the surface is described by a distribution function $\rho(E_{ads})$,[15] which expresses the total number of sites (N) corresponding to the activation energy level from E_{ads} and $E_{ads} + dE_{ads}$:

$$\rho(E_{ads}) = \frac{1}{N}\frac{dN(E_{ads})}{dE_{ads}} \quad (13)$$

If $\theta_{t,Eads}$ represents the fraction of sites with energies between E_{ads} and $E_{ads} + dE_{ads}$ occupied by adsorption in the time t, the fraction of the entire surface θ_t, occupied at a certain time t can be calculated using eq 14.

$$\theta_t = \int_{E_{min}}^{E_{max}} \theta_{t,Eads}\rho(E_{ads})dE_{ads} \quad (14)$$

As no interaction between the adsorbed compounds is considered, the adsorption kinetics for sites of equal activation energy are governed by the same Langmuirian expression:

$$\frac{d\theta}{dt} = k_a \exp\left(\frac{-E_{ads}}{RT}\right)C(1-\theta_t) - k_d \exp\left(\frac{-E_{des}}{RT}\right)\theta_t \quad (15)$$

with k_a and k_d the rate constant of, respectively, adsorption and desorption, C the feed concentration, R the universal gas constant, and T the temperature in Kelvin.

If $r_{ads} \gg r_{des}$, the surface coverage $\theta_{t,Eads}$ corresponding with an activation energy E_{ads} at a given time t can be found by integration of eq 15.

$$\theta_{t,Eads} = 1 - \exp\left[-Ctk_a \exp\left(\frac{-E_{ads}}{RT}\right)\right] \quad (16)$$

For a given constant concentration at a given time t, all adsorption sites from the lowest activation energy E_{ads} upward to a specific activation energy E_{ads} are effectively completely occupied ($\theta_{t,Eads} > 0.99$). Sites with a slightly higher adsorption energy form a working band, containing those values of E_{ads} for which the degree of surface coverage ranges at time t_1 from 0.01 to 0.99. Finally, sites with an even greater adsorption energy are completely unoccupied ($\theta_{t,Eads} < 0.01$). At a time t_2, the working band shifts toward higher adsorption energy values. The degree of overall surface coverage can be obtained by integration of eq 16.

Several authors tried to derive the adsorption kinetics to describe adsorption at a heterogeneous surface, assuming that the particles do not interact. The Rogiskii procedure that corresponds to the assumption that sites are distributed equally according to their activation energy, is the most generally applicable one. It is true that the Rogiskii method is only approximate, but its precision is quite satisfactory. Moreover, the method is simple and straightforward. Therefore, the Roginskii approximation is used. This means that the limit that separates the occupied and unoccupied sites is represented by a vertical boundary which sharply separates $\theta_{t,Eads} = 0$ from those with $\theta_{t,Eads} = 1$ at the inflection point E_{inf} (Figure 1).

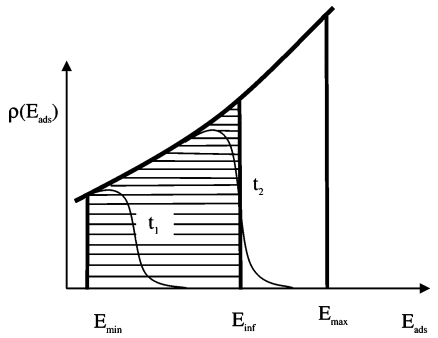

Figure 1. Distribution of adsorption sites according to their activation energies. The shaded area corresponds to integral 12.

Using this approximation method, eq 14 is simplified into eq 17. The less steep the function $\rho(E_{ads})$, the more accurate the approximation.

$$\theta_t = \int_{E_{min}}^{E_{inf}} \rho(E_{ads})\, dE_{ads} \quad (17)$$

Rogiskii et al.[15] obtained an expression for E_{inf} by putting the second derivative of $\theta_{t,Eads}$ to E_{ads} equal to 0. K represents the integration constant, which is concentration (C) dependent.

$$E_{inf} = K(C) + RT\ln t \quad (18)$$

Assuming that the sites are distributed equally according to their activation energy, i.e., $\rho(E_{ads})$ is equal to the constant H, the following expression of θ is obtained:

$$\theta = H\int_{E_{min}}^{E_{inf}} dE_{ads} = HRT\ln t = \beta\ln(t+\tau_0) - \beta\ln\tau_0 \quad (19)$$

The parameter τ_0 was introduced to justify the adsorption behavior for $t \to 0$. At $t = 0$, membrane and feed solution are brought into contact. Organic compounds in the solution need to diffuse to the membrane surface before interactions between membrane and compound are possible and thus before adsorption on the membrane can occur. Therefore, θ represents the surface fraction covered by the adsorption process which sets in at τ_0. The parameter β equals the product of temperature, gas constant, and distribution of energy sites and represents the number of sites that are available for adsorption. A high value of H corresponds to a high number of sites that are available.

Flux Decline as a Function of Time. Adsorption of organic compounds results in a reduction of the available pores because the pores will become blocked. Nanofiltration membranes generally have a rather dense structure and the pores can be seen as the free volume between the polymer chains of the membrane (= "nanopores"). These nanopores have a size in the same order as the size of the organic molecules in the feedwater. However, an organic molecule can only enter the pore if its size is smaller than the pore size (sieving). This means that a fraction of the theoretical adsorption sites in the membrane (in the nanopores) will not be available for the organic molecules, and therefore a complete monolayer coverage of the membrane surface (theta = 1) is impossible. Adsorption can

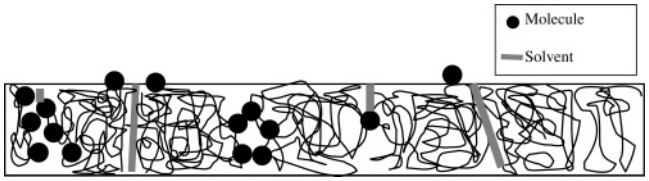

Figure 2. Different mechanisms of pore blocking during nanofiltration of organic compounds.

occur when the pore and molecular size are almost the same. In this case adsorption of one molecule already results in pore blocking and thus flux decline (= less than monolayer coverage). Previous research already showed that flux decline is the highest when molecule and pore size are comparable.[16] When the pore size is larger compared to the molecular size, the pore size will be reduced by adsorption which finally also results in pore blocking. The different mechanisms are represented in the Figure 2.

Adsorption causes thus a reduction of the pure water permeability (L_{P0}) with a factor ($= K < 1$) proportional to the number of occupied sites (θ). The factor K is also introduced because otherwise the permeability would become zero if all adsorption sites are occupied. However, organic molecules cannot enter the pores which have a size smaller than their molecular size. Therefore, a fraction of the adsorption sites is not available due to this sterical hinder effect. Finally, the water permeability (L_P) becomes:

$$L_P = L_{P0}(1-K\theta) \tag{20}$$

Based on adsorption thermodynamics, a logarithmic function of time (eq 17) was obtained for the fraction of occupied sites (θ), resulting in

$$L_P = L_{P0}(1 - b\ln(t + t_0) + b\ln t_0) \tag{21}$$

Using this expression of L_P in the Spiegler−Kedem[17] equations, a logarithmic decrease of the normalized flux (J) as a function of time is predicted:

$$J = L_{P0}(1 - b\ln(t + t_0) + b\ln t_0)(\Delta P - \sigma\Delta\pi) \tag{22}$$

To verify the correlation between flux (J) and time (t), the equation was rewritten:

$$1 - \frac{J}{L_{P0}(\Delta P - \sigma\Delta\pi)} = b\ln(t + t_0) - b\ln t_0 \tag{23}$$

The left side of eq 23 represents the normalized flux decline (ΔJ), which was defined in eq 22 using the definition of the pure water flux J_0 (eq 25):

$$\Delta J = 1 - \frac{J}{J_0} \tag{24}$$

$$J_0 = L_{P0}(\Delta P - \sigma\Delta\pi) \tag{25}$$

The parameter b refers to the reduction of free volume due to adsorption and is proportional with the number of available sites. However, one should not confuse b and β. β represents the available sites for adsorption of the organic compounds on the membrane, whereas b refers to the reduction of free (pore) volume due to adsorption, which is proportional to the number of available sites ($K\beta$) because not all adsorption sites should be occupied before pores become blocked and not all adsorption sites will be available due to sieving effects. Therefore, β and b are not the same parameters.

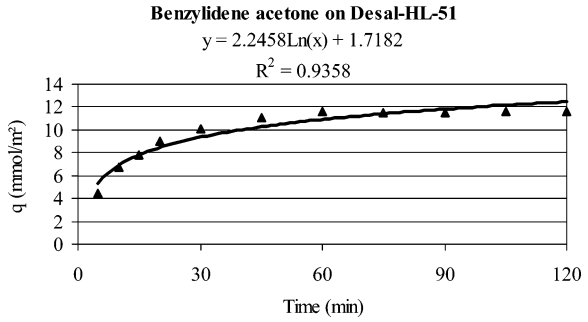

Figure 3. Adsorbed mass (q) as a function of time ($t + \tau_0$) for benzylidene acetone on Desal-HL-51.

The parameter t_0 represents the time at which adsorption results in effective pore blocking and thus a reduction of the water flux. Molecules not only need to diffuse to the membrane surface, they should also enter the "pores" were they can adsorb, resulting in a reduction of the free volume and thus flux decline.

4. Results and Discussion

Adsorbed Mass on the Membrane as a Function of Time. Surface coverage as a function of time for polymeric nanofiltration membranes was investigated by measuring the adsorbed amount on the surface (q) as a function of time ($t + t_0$).

Figure 3 represents the adsorption of benzylidene acetone on Desal-HL-51. A logarithmic correlation was found with a R^2 value of 0.9737. Similar results were obtained for NTR 7450 and UTC-20 using different organic compounds (e.g., 3,5-dihydroybenzoic acid, 3,4 methylnitrophenol and benzylidene acetone). The rate of adsorption and desorption was determined in adsorption and desorption experiments as a funtion of time. The rate was calculated as the difference in adsorbed (desorbed) amount during a short time period (∼5 min). The ratio of adsorption rate to desorption rate ranges between 50 and 90, which confirms the assumption that $r_{ads} \gg r_{des}$.

Flux Decline as a Function of Time. The reflection coefficient (σ) was equilized to the retention of the compounds at 8 bar. A good agreement between reflection coefficient and retention was obtained in previous studies.[18] The osmotic pressure ($\Delta\pi$) was calculated by the Van't Hoff equation:

$$\Delta\pi = \nu c_j RT \tag{26}$$

with ν the Van't Hoff factor, c_j the feed concentration (mol L^{-1}), R the gas constant and T the temperature (K).

The normalized flux decline for benzylidene acetone (2 mmol L^{-1}), 3,5-dihydroxybenzoic acid (5 mmol L^{-1}), and 3,4-methylnitrophenol (5 mmol L^{-1}) on three membranes (Desal-HL-51, NF210 and UTC-20) are represented in Figure 4. The R^2 values were all above 0.95. Similar correlations were obtained for the other hydrophobic compounds. Modeling flux decline of hydrophilic compounds (triethylene glycol and tartaric acid) was less successful due to the fact that these compounds do not adsorb significantly. The R^2 values of triethylene glycol and tartaric acid range between 0.51 and 0.85.

It could be concluded that, for hydrophobic organic compounds, a modification of the Spiegler−Kedem equation, incorporating the influence of adsorption on the membrane, results in a good description of the flux as a function of time.

Estimation of Model Parameters. Two parameters were used in the model. The parameter t_0 corresponds to actual time on which pore size reduction due to adsorption occurs and the

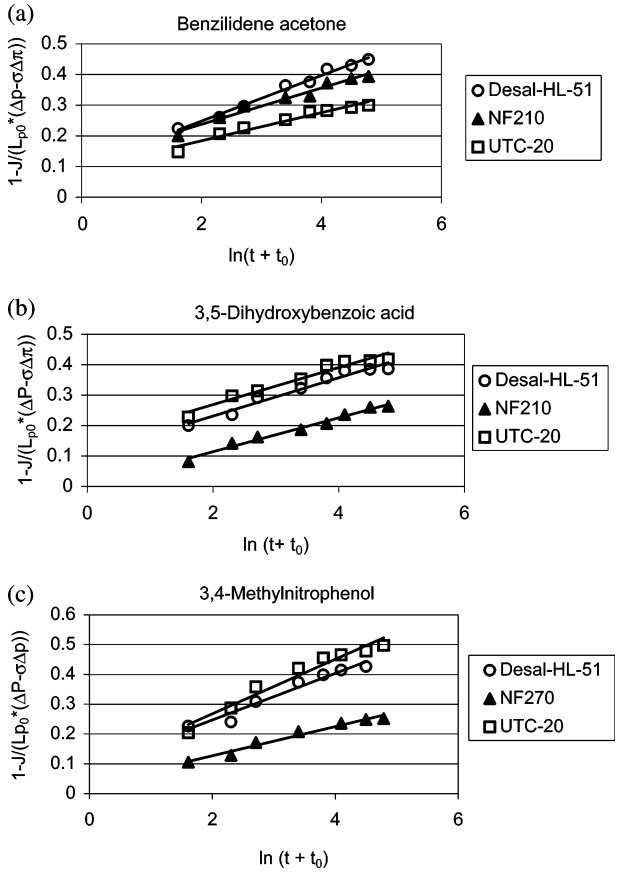

Figure 4. Normalized flux decline $[1 - (J/(L_{P0}(\Delta P - \sigma\Delta\pi))]$ of (a) benzylidene acetone (2 mmol L^{-1}), (b) 3,5-dihydroxybenzoic acid, and (c) 3,4-methylnitrophenol (5 mmol l^{-1}) as a function of $\ln(t + t_0)$.

normalized flux starts to decrease. The parameter *b* corresponds to the distribution of available sites of the adsorption process and represents the reduction of free (pore) volume due to adsorption. Both parameters were calculated based on flux decline measurements of 11 different compounds (triethylene glycol, diethanolamine, diethylene glycol, tartaric acid, 3,5 dihydroxybenzoic acid, cyclohexanone, benzonitrile, benzaldehyde, benzylidene acetone, *p*-tolualdehyde, and 3,4-methylnitrophenol). The obtained values also depend on the membrane used in the experiment.

Adsorption occurs relatively quickly for hydrophobic compounds resulting in a stable normalized flux. However, it is difficult to determine the exact equilibrium time.Therefore, the curves during two different periods were determined. Initially, *b* and t_0 were calculated from the slope and intercept of the curve using the data points at 5, 10, 15, and 30 min, assuming thus an equilibrium time of 30 min.

Second, an equilibrium time of 120 min was assumed. In this case, *b* and t_0 were obtained from a curve using the data at 5, 10, 15, 30, 45, 60, 90, and 120 min. Both values for *b* and t_0 were indicated in the following figure; the average of both is represented by the data point in Figures 5 and 6. The obtained range was indicated only if maximum and minimum values differ 5% or more of the average value.

Figure 5 represents the values of *b* as a function of log *P* on Desal-HL-51 and NF270. It can be concluded that a high value of log *P* corresponds to a high value of *b*, representing a high reduction of the free pore volume due to adsorption of hydrophobic compounds on the membrane. The more hydrophilic the compounds, the less reduction occurs due to adsorption; a low value of *b* is obtained. It is expected that the

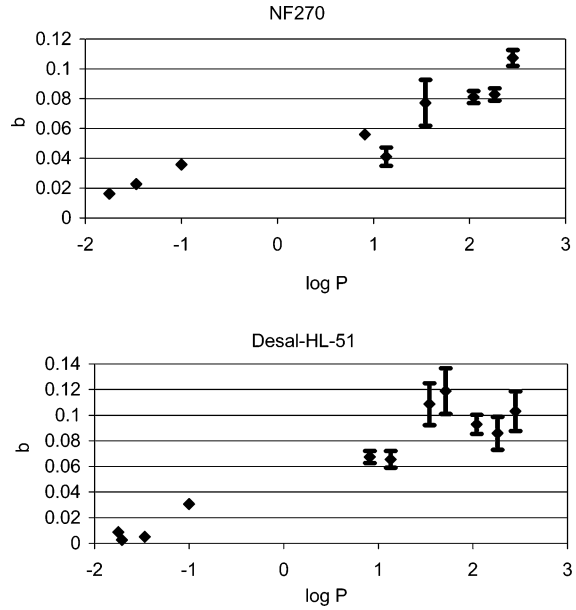

Figure 5. *b* as a function of log *P*.

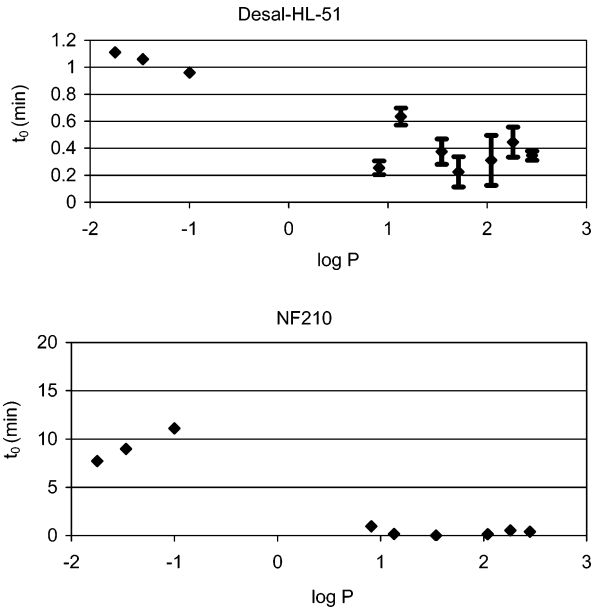

Figure 6. t_0 (min) as a function of log *P*.

molecular size of the organic compounds might also influence reduction of pore size. However, in a first approach, only the hydrophobicity of the compounds was taken into account by using molecules with a comparable molecular weight.

Figure 6 shows the correlation between t_0 and log *P*. Generally, it can be concluded that a reduction of free pore volume (and thus flux decline) due to adsorption of hydrophobic compounds occurs quickly resulting in a small time delay (small value of t_0). The less hydrophobic the organic compound, the longer it takes before a significant pore size reduction is obtained resulting in flux decline. This can be seen from Figure 6 where t_0 is always higher for the hydrophophilic compounds (left-hand side, log $P < 0$) than for the hydrophobic compounds (right-hand side, log $P > 0$). The scattering on the trend can be explained by a difference in molecular size between the different molecules which might also influence the effectivity of adsorption and the reduction of pore size.

Influence of Feed Concentration on Model Parameters. The influence of concentration on *b* and t_0 was studied by

TABLE 4: Model Parameters b and t_0 at Different Feed Concentrations

feed conc.	Desal-HL-51		UTC-20		NTR7450		NF270	
(mmol/L)	b	t_0	b	t_0	b	t_0	b	t_0
				3,5-dihydroxybenzoic acid				
2	0.050	0.30	0.054	1.81	0.063	3.67	0.033	0.35
5	0.067	0.26	0.065	0.12	0.088	3.06	0.057	1.01
10	0.113	0.21	0.126	0.13	0.125	2.07	0.083	0.19
				3,4-methylnitrophenol				
2	0.053	0.92	0.024	0.74	0.081	0.69	0.063	0.96
5	0.104	0.35	0.054	0.02	0.147	1.63	0.107	0.66
				benzylidene acetone				
2	0.076	0.31	0.052	0.31	—[a]	—[a]	0.065	0.20
5	0.093	0.29	0.068	0.23	—[a]	—[a]	0.081	0.17

[a] No data available.

TABLE 5: Relative Fault (δ) on b and t_0

feed conc.	Desal-HL-51		UTC-20		NTR7450		NF270	
(mmol/L)	δb	$\delta(\ln t_0)$	δb	$\delta(\ln t_0)$	δb	$\delta(\ln t_0)$	δb	$\delta(\ln t_0)$
				3,5-dihydroxybenzoic acid				
2	0.02	0.282	0.04	0.714	0.03	0.829	0.01	0.265
5	0.02	0.260	0.02	0.135	0.02	0.175	0.01	0.730
10	0.02	0.208	0.01	0.136	0.03	0.322	0.01	0.164
				3,4-methylnitrophenol				
2	0.03	0.129	0.02	0.044	0.01	0.412	0.06	0.980
5	0.02	0.668	0.05	0.330	0.02	0.660	0.11	0.410
				benzylidene acetone				
2	0.01	3.2E−05	0.02	4.1E−05	—[a]	—[a]	0.01	4.3E−05
5	0.01	4.9E−05	0.02	9.3E−05	—[a]	—[a]	0.01	5E−05

[a] Data not available.

filtration of feed solutions with different concentrations as is represented in Table 4 for 3,5-dihydroxy benzoic acid, 3,4-methylnitrophenol, and benzylidene acetone on four different membranes. The relative errors on both parameters are summarized in Table 5.

It can be concluded from Table 4 that with increasing feed concentration, the pore volume reduction due to adsorption (b) increases. This decrease depends on both membrane and compound. The highest value is generally obtained for the NTR7450 membrane, which is a polyethersulfon membrane and more hydrophobic than the other three membranes, which are polyamide membranes.

The increase in b also depends on the compounds: 3,4-methylnitrophenol ($\log P = 2.45$) and benzylidene acetone ($\log P = 2.04$) generally obtain higher values of b than 3,5-dihydroxybenzoic acid ($\log P = 0.91$). This difference is more significant at higher concentrations. Finally, the change of b also depends on the compound: only a slight increase was noticed for benzylidene acetone, whereas b almost doubles for 3,4-methylnitrophenol with increasing concentration.

This can be explained by an increased number of sites which will be occupied at higher concentration at a certain time, as was also indicated by Freundlich and Langmuir isotherms,[19] resulting in a higher amount of blocked pores. Generally, the time delay (t_0) also decreased at increasing feed concentration except for 3,4-methylnitrophenol at NTR-7450 and 3,5-dihydroxybenzoic acid at NF270, indicating that significant pore size reduction occurs earlier in the filtration process.

5. Conclusions

A logarithmic correlation between flux decline and time was obtained by implementing the reduction of pore size due to adsorption in the Spiegler−Kedem equation for solvent transport. The reduction of pore volume due to pore blocking (b) and the time delay (t_0) depend both on the hydrophobicity of the compounds: for hydrophilic compounds (small value of log P) a small value of b is obtained (<0.04) and b increases with increasing log P. For high value of log P (> 1.5), b ranges between 0.08 and 0.12. The adsorption of a hydrophobic compound also results quickly in a significant flux decline (low value of t_0). Increasing the feed concentration results in an increase of pore size reduction.

Acknowledgment. L.B. is grateful to the IWT (Vlaams Instituut voor de bevordering van Wetenschappelijk-Technologisch onderzoek in de industrie) for a PhD grant. We thank Toray Ind. Inc., Nitto-Denko and Dow/Filmtec for kindly supplying respectively the UTC-20 membrane, the NTR 7450 membrane and the NF270 membrane.

References and Notes

(1) Everest, W. R.; Malloy, S. *Desalination* **2000**, *117*, 149.
(2) Gorenflo, A.; Velazquez-Padron, D.; Frimmel, F. H. *Desalination* **2003**, *151*, 253.
(3) Cyna, B.; Chagneau, G.; Bablon, G.; Tanghe, N. *Desalination* **2002**, *147*, 69.
(4) Braeken, L.; Ramaekers, R.; Zhang, Y.; Maes, G.; Van der Bruggen, B.; Vandecasteele, C. *J. Membr. Sci.* **2005**, *252*, 195.
(5) Schäfer, A. I.; Fane, A. G.; Waite, T. D. *Desalination* **2000**, *131*, 215.
(6) Kimura, K.; Amy, G.; Drewes, J.; Watanabe, Y. *J. Membr. Sci.* **2003**, *221*, 89.
(7) Van der Bruggen, B.; Braeken, L.; Vandecasteele, C. *Sep. Purif. Technol.* **2002**, *29*, 23.
(8) Kiso, Y.; Kitao, T.; Nishimura, K. *J. Appl. Polym. Sci.* **1999**, *71*, 1657.
(9) Kiso, Y.; Kitao, T.; Nishimura, K. *J. Appl. Polym. Sci.* **1999**, *74*, 1037.
(10) Van der Bruggen, B.; Braeken, L.; Vandecasteele, C. *Desalination* **2002**, *147*, 281.
(11) Kilduff, J. H.; Mattaraj, S.; Belfort, G. *J. Membr. Sci.* **2004**, *239*, 39.
(12) Li, Q. L.; Elimelech, M. *Environ. Sci. Technol.* **2004**, *38*, 4683.
(13) Schaep, J.; Vandecasteele C. *J. Membr. Sci.* **2001**, *188*, 129.
(14) Eisenberg M.; Gresalfi T.; Riccio T.; McLaughlin S. *Biochemistry* **1979**, *18*, 5213.
(15) Ponec, V.; Knor, Z.; Cerny, S. In *Adsorption on solids*; Butterworth: London, 1974; Chapter 8.
(16) Van der Bruggen, B.; Braeken, L.; Vandecasteele C. *Desalination* **2002**, *147*, 281.
(17) Spiegler, K. S.; Kedem, O. *Desalination* **1996**, *1*, 311.
(18) Van der Bruggen, B.; Schaep, J.; Vandecasteele, C.; Wilms, D. *Sep. Purif. Technol.* **1999**, *35*, 169.
(19) Braeken, L.; Boussu, K.; Van der Bruggen, B.; Vandecasteele, C. *ChemPhysChem* **2005**, *6*, 1606.